Environmental Pollution 220 (2017) 616–624

Contents lists available at ScienceDirect

Environmental Pollution

journal homepage: www.elsevier.com/locate/envpol

Benzotriazole UV 328 and UV-P showed distinct antiandrogenic activity upon human CYP3A4-mediated biotransformation☆

Shulin Zhuang [a, b, *], Xuan Lv [a, c], Liumeng Pan [a], Liping Lu [a], Zhiwei Ge [a], Jiaying Wang [a], Jingpeng Wang [a], Jinsong Liu [d], Weiping Liu [a], Chunlong Zhang [e, **]

[a] Institute of Environmental Science, College of Environmental and Resource Sciences, Zhejiang University, Hangzhou 310058, China
[b] Key Laboratory of Health Risk Factors for Seafood of Zhejiang Province, Zhoushan 316022, China
[c] Guangzhou Key Laboratory of Environmental Exposure and Health, School of Environment, Jinan University, Guangzhou 510632, China
[d] Zhejiang Province Environmental Monitoring Center, Hangzhou 310005, China
[e] Department of Biological and Environmental Sciences, University of Houston-Clear Lake, 2700 Bay Area Blvd., Houston, TX 77058, USA

ARTICLE INFO

Article history:
Received 24 July 2016
Received in revised form
30 September 2016
Accepted 4 October 2016
Available online 13 October 2016

Keywords:
Benzotriazole UV stabilizers
Androgen receptor
Metabolism
Molecular modeling
Mass spectrometry

ABSTRACT

Benzotriazole ultraviolet stabilizers (BUVSs) are prominent chemicals widely used in industrial and consumer products to protect against ultraviolet radiation. They are becoming contaminants of emerging concern since their residues are frequently detected in multiple environmental matrices and their toxicological implications are increasingly reported. We herein investigated the antiandrogenic activities of eight BUVSs prior to and after human CYP3A4-mediated metabolic activation/deactivation by the two-hybrid recombinant human androgen receptor yeast bioassay and the *in vitro* metabolism assay. More potent antiandrogenic activity was observed for the metabolized UV-328 in comparison with UV-328 at 0.25 μM ((40.73 ± 4.90)% vs. (17.12 ± 3.00)%), showing a significant metabolic activation. In contrast, the metabolized UV-P at 0.25 μM resulted in a decreased antiandrogenic activity rate from (16.08 ± 0.95)% to (6.91 ± 2.64)%, indicating a metabolic deactivation. Three mono-hydroxylated (OH) and three di-OH metabolites of UV-328 were identified by ultra-performance liquid chromatography quadrupole time of flight mass spectrometry (UPLC-Q-TOF-MS/MS), which were not reported previously. We further surmised that the hydroxylation of UV-328 occurs mainly at the alicyclic hydrocarbon atoms based on the *in silico* prediction of the lowest activation energies of hydrogen abstraction from C-H bond. Our results for the first time relate antiandrogenic activity to human CYP3A4 enzyme-mediated hydroxylated metabolites of BUVSs. The biotransformation through hydroxylation should be fully considered during the health risk assessment of structurally similar analogs of BUVSs and other emerging contaminants.

1. Introduction

Benzotriazole ultraviolet stabilizers (BUVSs) are one prominent group of (2-hydroxyphenyl) benzotriazole derivatives used to protect against ultraviolet radiation from sunlight (Table 1). They have been widely used as UV light stabilizers, anticorrosive and antifogging agents incorporated in multiple industrial materials, coated textiles and daily commodities (Ruan et al., 2012; LeFevre et al., 2015). BUVSs are listed in the High Production Volume (HPV) Challenge Program by the U.S. EPA and the OECD (Ruan et al., 2012). Due to the high volume production and widespread usage, the residues of BUVSs have been detected in indoor air dust (Wang et al., 2013), river sediment (Nakata et al., 2009; Kameda et al., 2011; Wick et al., 2016), wastewater (Liu et al., 2012, 2014), sea food (Kim et al., 2011), human breast milk (Kameda et al., 2011), human adipose tissue (Wang et al., 2015) and human urine (Asimakopoulos et al., 2013a,b). The exposure to BUVSs has raised increasing public concern, however, research needed to determine the potential risk on human and ecosystems falls behind the production and wide usages of BUVSs already in place. BUVSs have a relatively low acute toxicity to aquatic organisms (Seeland et al., 2012) and no estrogenic activities in yeast two-hybrid assay (Kawamura et al., 2003; Morohoshi et al., 2005; Miller et al., 2001). However, BUVSs exerted estrogenic potential in marine medaka at

☆ This paper has been recommended for acceptance by Charles Wong.
* Corresponding author. Institute of Environmental Science, College of Environmental and Resource Sciences, Zhejiang University, Hangzhou 310058, China.
** Corresponding author.
E-mail addresses: shulin@zju.edu.cn (S. Zhuang), zhang@uhcl.edu (C. Zhang).

http://dx.doi.org/10.1016/j.envpol.2016.10.011
0269-7491/

Table 1
Structures of the tested benzotriazole UV stabilizers (BUVSs).

Compound	CAS No.	Structure
UV-P	2240-22-4	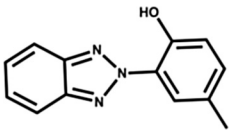
1H-BT	95-14-7	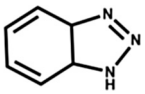
UV-234	70321-86-7	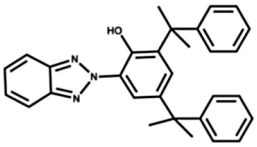
UV-326	3896-11-5	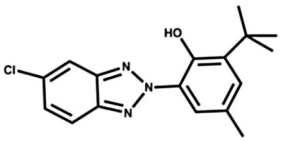
UV-327	3864-99-1	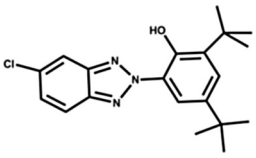
UV-328	25973-55-1	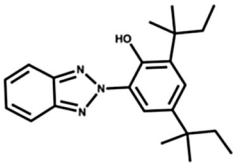
UV-329	3147-75-9	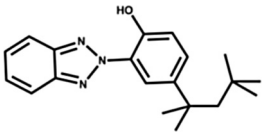
UV-350	36437-37-3	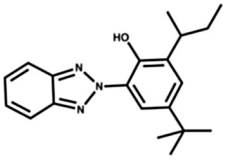

environmentally relevant concentrations (~0.01 mg/L) (He et al., 2012) and 1H-benzotriazole (1HBT) was shown to have anti-estrogenic properties (Harris et al., 2007). UV-P and 1HBT exerted antagonistic activity toward androgen receptor (AR) (Fent et al., 2014; Nagayoshi et al., 2015). UV-P, UV-9, UV-326 and UV-090 were reported to have activities toward aryl hydrocarbon receptor (AhR) and UV-P and UV-326 were involved in the AhR pathway in zebrafish embryos (Fent et al., 2014).

These reported studies on the biological effects of BUVSs did not address whether such effects can be affected by their transformation. BUVSs are known to be transformed in the environment or biota. Three BUVSs (1H-BT, 4-CH3-BT and 5-CH3-BT) were reportedly degraded by microorganisms in activated and digested sludge under both aerobic and anaerobic conditions (Huntscha et al., 2014; Liu et al., 2011). 1HBT and 2-mercaptobenzothiazole (MBT) were recently shown to be rapidly phytotransformed by an *Arabidopsis* plant into metabolites structurally resembling auxin and tryptophan plant hormones, or glucose and amino conjugated MTB metabolites (LeFevre et al., 2015, 2016). The toxicological significance of these transformation products is not exactly known, but several transformation products were reported to have increased toxicities after the metabolic activation by the xenobiotic metabolizing enzymes. For example, bisphenol A was metabolically activated for its estrogenicity by rat liver S9 (Yoshihara et al., 2001), and the metabolism of polybrominated diphenyl ethers (PBDE) by CYP450 resulted in hydroxylated products with an increased thyroid hormone disrupting potency (Li et al., 2010; Zhang et al., 2015). A recent study revealed that human CYP1A1 enzyme also deactivated certain BUVSs (UV-P, UV-9 and UV-090) toward AhR (Nagayoshi et al., 2015; LeFevre et al., 2016). Despite this important finding, very limited work has been performed to date to study the biotransformation of BUVSs (including the identification of the potential metabolites) and elucidate whether the antiandrogenic activities of these BUVSs could be activated via biotransformation.

In the present study, we evaluated human CYP3A4-mediated metabolic activation/deactivation of UV-P, 1HBT, UV-234, UV-326, UV-327, UV-328, UV-329 and UV-350 (Table 1) and identified several prominent metabolites capable of higher antiandrogenic activities. The metabolic activation of BUVSs was screened by using an *in vitro* metabolism bioassay. The hydroxylated metabolites were identified by ultra-performance liquid chromatography coupled with quadrupole time of flight mass spectrometry (UPLC-Q-TOF-MS/MS). Sites of metabolism (SoM) were predicted by the evaluation of reactivity of hydrogen abstraction from C-H bond. To the best of our knowledge, this is the first report on the metabolic activation/deactivation of BUVSs. Results on the metabolic activation/deactivation should be fully incorporated into the risk assessment of these emerging contaminants.

2. Material and methods

2.1. Materials

Dihydrotestosterone (DHT, 99%, CAS No. 521-18-6) and dimethylsulfoxide (DMSO, 99.5%) were purchased from Sigma Chemical Company (St. Louis, MO, USA). 2-(Benzotriazol-2-yl)-4-methylphenol (UV-P, 98%, CAS No. 2440-22-4) and 2-(2′-hydroxy-3′,5′-di-*tert*-amylphenyl) benzotriazole (UV-328, 99%, CAS No. 25973-55-1) were purchased from J&K Chemical Ltd. (Shanghai, China). SD/-Leu/-Trp medium was obtained from Mobitec Company (Catalogue: 4823-6). Human liver microsome pooled donors (HLM, 20 mg/mL, Catalogue: 452161), P450-Glo™ CYP3A4 assay (Catalogue: v9001, Shanghai Promega Biological Products, Ltd., China), human cytochrome 3A4 (Catalogue: 456202) and NADPH system (Solution A, Catalogue 451220; Solution B, Catalogue 451200) were all purchased from BD Biosciences Company (Shanghai, China). Other chemicals were of analytical grade. All test chemicals were dissolved in DMSO (v/v < 0.1%) and the corresponding stock solutions were prepared with Milli-Q water (18.2 MΩ, Millipore, Bedford, MA).

2.2. Two-hybrid recombinant yeast bioassay

The disrupting activities of BUVSs towards AR were determined by the two-hybrid recombinant yeast bioassay using the yeast strain Y187. The yeast *Saccharomyces cerevisiae* was stably transfected with pGBT9 AR plasmids coding human AR ligand-binding domain (LBD) and LacZ reporter gene encoding the enzyme β-galactosidase (Li et al., 2008; Ma et al., 2005). pGBT9 AR plasmid was provided by Dr. Erik Jan Dubbink (Erasmus University, Holland)

and the two-hybrid recombinant yeast strain was provided by Prof. Zijian Wang (Research Center for Eco-Environmental Sciences, Chinese Academy of Sciences, Beijing, China). The yeast strain was preincubated at 30 °C and grew on the SD/-Leu/-Trp medium overnight. 5 μL of test chemicals and 995 μL medium containing 5×10^3 yeast cells/mL were mixed to make a test culture. The culture was preincubated at 30 °C for 2 h and was then treated following reported protocols (Ma et al., 2005). The enzyme reaction was initiated by adding *o*-nitrophenyl-β-D-galactopyranoside to the yeast cell lysates and was terminated after 60 min by adding 100 μL sodium carbonate (1 M). The absorbance at 420 nm was then measured by Infinite 200 PRO NanoQuant Multimode Microplate Reader (Tecan Group Ltd., Switzerland) and the β-galactosidase activity of tested chemicals was then calculated.

2.3. Metabolic incubation

The metabolism of BUVSs by HLM or CYP3A4 enzyme was conducted in Eppendorf tubes following established protocols (Lu et al., 2013). 10 μL BUVSs, 50 μL solution A and 10 μL solution B was mixed with 90 μL pooled HLM (0.9 mg/mL) or human CYP3A4 enzyme (0.1 pmol) as well as potassium phosphate buffer (110 mM, pH 7.4). The mixture with a total volume of 1 mL was incubated at 37 °C for 150 min. Reactions were terminated with 1 mL of ice-cold methanol and the incubation mixture was immediately centrifuged with a speed of 10,000 rcf for 15 min at 4 °C. The supernatant was collected in 1.5 mL Eppendorf tube and stored at −20 °C for further two-hybrid recombinant yeast bioassay. The incubation system without HLM or CYP3A4 was used as the negative control. All incubation experiments were performed in triplicate.

2.4. In silico prediction of the site of metabolism

Due to the lack of commercially available standards of potential metabolites, the site of metabolism (SoM) of BUVSs was predicted by SMARTCyp V2.4.2, the established cytochrome P450-mediated metabolism prediction server using the reactivity model (Rydberg et al., 2010). The SoM prediction from SMARTCyp was further validated by the evaluation of the activation energy of hydrogen abstraction.

We used density functional theory (DFT) method to investigate hydrogen abstraction by Compound I (Cpd I) in cytochrome P450. The Cpd I was represented by the model six-coordinate tri-radicaloid oxo-ferryl complex Fe4+O2-(C20N4H12)-1(SH)-1(Olsen et al., 2006). The initial geometry optimizations of BUVSs, Cpd I and their transition state (TS) and relevant frequency calculations were performed using the unrestricted hybrid UB3LYP method. The Fe atom was treated with double-ζ LanL2DZ (Fe) basis set and the other atoms with 6-31G** basis set. The single point energies were calculated at the UB3LYP/6-311++G** level. The solvent effect of water was evaluated using the integral equation formalism polarizable continuum model (IEF-PCM). The zero-point vibrational energy was included during the calculation of activation energy. Gaussian 09 program was used for all calculations.

2.5. UPLC-Q-TOF-MS/MS analysis

A 1-mL mixture containing 0.3 μM UV-328, 90 μL HLM (final concentration: 0.12 mg/mL) and 60 μL NADPH was incubated at 37 °C for 2 h. A 10 μL resultant supernatant of the incubation mixture was analyzed by electrospray ionization-Q-TOF-MS/MS method using TripleTOF 5600+system (AB SCIEX, Framingham, USA) coupled with Waters ultra-performance liquid chromatography (UPLC) (Waters Corp., Milford, MA, USA). The liquid supernatant was injected to UPLC and analytes were separated by ZorBax SB-C_{18} reverse phase column (2.1 mm × 100 mm, 3.5 μm, Agilent) with a flow rate of 0.5 mL/min. Mobile phases A and B were 0.1% formaldehyde (FA) in water and 0.1% FA in acetonitrile. The initial gradient of 30% B was used, followed by a gradient toward 100% B within 30 min, then 100% B for 35 min. The IDA-based auto-MS2 was performed on the 8 most intense metabolite ions in a cycle of full scan (0.94 s). The scanning range for ESI-Q-TOF-MS was set at 100–1500 m/z. The positive ion mode was set with a source voltage of +5.5 kV and the source temperature of 600 °C. The pressure of Gas 1 (Air) and Gas 2 (Air) were set to 50 psi, and the pressure of Curtain Gas (N_2) was set to 30 psi. The detection wavelength was set at 254 nm with the maximum allowed error of ±5 ppm. The collision energy was set at 40 V with a collision energy spread of ±20 V. The Automated Calibration Delivery System was applied for the exact mass calibration. The relevant fragmentation pathways were predicted by MetabolitePilot™ version 1.5 (AB SCIEX, Framingham, USA) based on the high-resolution molecular masses. The full-scan mass spectral data were processed and the extracted ion chromatograms (EICs) were calculated based on the predicted metabolite ions.

2.6. Statistical analysis

The dose-response curve obtained from the two-hybrid recombinant yeast bioassay was fitted employing Levenberg-Marquardt algorithm by IBM SPSS Statistics 20. The obtained values were given as mean ± standard deviation (SD). The cut-off *p*-value below 0.05 ($p < 0.05$) was considered as a significant difference.

3. Results

3.1. Antagonistic effect of BUVSs before human CYP3A4-mediated metabolism

Besides the disrupting effect of some BUVSs toward AhR, the androgenic disrupting effect of BUVSs has been the subject of several recent studies (Harris et al., 2007; Fent et al., 2014; Chen et al., 2016). In this work, the antagonistic activity of eight BUVSs (Table 1) was rapidly evaluated using the established two-hybrid recombinant human AR gene yeast bioassay (Fent et al., 2014; Li et al., 2011). The β-galactosidase activity of an endogenous AR agonist, dihydrotestosterone (DHT) was measured first and the standard dose-response curve of DHT was obtained with the maximum activity at 5×10^{-2} μM (Fig. S1). The IC_{50} was determined to be 5×10^{-3} μM, in line with reported studies (Fent et al., 2014; Li et al., 2011). The β-galactosidase activity of 8 BUVSs was measured by co-incubation of the yeast strain with 2×10^{-2} μM DHT. All BUVSs were diluted to the concentration of 5.0×10^{-5} ~ 50 μM for UV-P, 1HBT, UV-326, UV-327, UV-329, UV-350 and 5×10^{-4} ~ 50 μM for UV-234 and UV-328. No toxicity to yeast cells was induced within this concentration range. The concentrations of BUVSs have been reported to be varies from ng/L to sub-ug/L in water and ug/g in aquatic organisms (Buser et al., 2006; Kameda et al., 2011; Tsui et al., 2014). The dose level in our experiments is within or very close to the reported environmental exposure levels and is therefore environmentally relevant. As shown in Fig. S2 (A), these BUVs did not induce the β-galactosidase activity in comparison with the solvent control, indicating that they are not agonists of human AR. The antagonistic activity of BUVSs was represented as the percentage of β-galactosidase activity in the presence of BUVSs to the activity observed at 5×10^{-2} μM DHT (Fig. S2). UV-P exhibited potent antagonistic activity with IC_{20} of 0.365 μM. 1HBT, UV-234, UV-326, UV-327, UV-328, UV-329 and UV-350 had no significant antiandrogenic activity at concentrations ranging from

5×10^{-5} μM to 5 μM; however, they showed weak antagonistic toxicity at a higher concentration (50 μM). Fent et al. have investigated the hormonal activity of UV-320, UV-326, UV-327, UV-328, UV-329, UV-P and 1HBT and their effects on zebrafish (Fent et al., 2014). They found no androgenic activity for these BUVSs at concentrations ranging from 10^{-7} to 1 g/L. However, UV-P and 1HBT exhibited the antagonistic activity at concentration higher than 1 μM and 100 μM, respectively (Fent et al., 2014). Minor structural differences among BUVSs may induce different antagonistic activities toward human AR.

3.2. Antiandrogenic effect of BUVSs after metabolism

A recent study revealed that certain BUVSs such as UV-P, UV-9, UV-326, and UV-090 have the AhR ligand activities and these activities remained unchanged in the presence of CYP1A1 (Nagayoshi et al., 2015). CYP3A4 is the predominant isoform among CYP450 family in liver and is also responsible for the metabolism of a large variety of exogenous and endogenous substrates. Thus, the metabolism of BUVSs by human CYP3A4 and its effects on androgenic effect of BUVSs is of significance. We investigated the effect of *in vitro* metabolism of eight BUVSs on their antiandrogenic activities (Fig. 1). Eight BUVSs were incubated for 2.5 h and the antiandrogenic effects of the incubation supernatant were tested using the two-hybrid recombinant human AR gene yeast bioassay. Since the test BUVSs showed no significant antiandrogenic effect at concentrations ranging from 5×10^{-5} μM to 1 μM (Fig. S2), three concentrations, 0.0025 μM, 0.025 μM, 0.25 μM was used to compare antiandrogenic effect before and after metabolism. The final concentration of UV-P and UV-328 with or without incubation with HLM was set the same.

As shown in Fig. 1, the metabolized products from both UV-P and UV-328 significantly altered the antagonistic activity. After CYP3A4-mediated metabolism, the inhibitory rate of UV-P at 0.25 μM was reduced from (16.08 ± 0.95)% to (6.91 ± 2.64)%, indicating a metabolic deactivation of UV-P. The inhibitory rate of UV-328 at 0.25 μM was increased from (17.12 ± 3.00)% to (40.73 ± 4.90)%, showing a significant metabolic activation. There are no significant differences ($p > 0.05$) in antiandrogenic activity before and after metabolism for six other BUVSs. We further evaluated the androgenic effect of UV-328 and UV-P after HLM-mediated metabolism (Fig. S3). At 0.25 μM, UV-328 after HLM-mediated metabolism showed a significant antiandrogenic activity in comparison with UV-328 before the metabolism. The inhibitory rate of UV-328 metabolites enhanced markedly from (27.95 ± 6.34)% to (43.28 ± 1.50)%. The inhibitory rate of UV-P metabolites was reduced from (24.23 ± 0.31)% to (17.93 ± 2.44)%. Bothe the human CYP3A4 and HLM-mediated metabolism consistently validated the metabolic activation/deactivation for UV-328 and UV-P.

3.3. UPLC-Q-TOF-MS/MS analysis of UV-328 metabolites

Among eight BUVSs, only UV-328 showed an enhanced antiandrogenic effect after the metabolism. It is thus necessary to identify the potential metabolites of UV-328. The supernatant of incubation mixture of UV-328 was analyzed by UPLC-Q-TOF-MS/MS. The relevant fragmentation pathways were predicted by MetabolitePilot™ version 1.5 (AB SCIEX, Framingham, USA) based on the high-resolution molecular masses (Table 2, Table S1). The % score of fragment ions indicates the possibility of a parent compound or its specific metabolite being present according to the accurate molecular mass. The metabolites with % score higher than 75% are all listed. The % signal area denotes the ratio of the molar mass of the detected compound to the total molar mass of UV-328. Four types of metabolism can be proposed, including hydroxylation, desaturation, demethylation and ketone formation and their % areas of the metabolites corresponding to these four pathways are 31.2%, 6.9%, 12.6%, and 13.8%, respectively. The hydroxylation is presumably the dominant metabolism pattern. UV-328 has a % score of 90.4% and all the hydroxylated metabolites have % score above 83%, showing the high possibility of the predicted metabolites being present. The mass spectrum revealed parent UV-328 and six hydroxylated metabolites (M5, M6, M11, M20, M21 and M24) (Fig. 2A, Fig. S4A). Compared with the m/z of UV-328 (352.239), the metabolites M20, M21 and M24 have an additional mass of 16 Da, indicating that these three metabolites are mono-OH metabolites (Table 2). The m/z of M5, M6 and M11 is 32 Da higher than that of UV-328, suggesting di-OH metabolites (Table 2, Table S2). We also carried out a parallel metabolism study on UV-328 by adding CYP3A4 inhibitor ketoconazole to HLM. The enzymatic activity of CYP3A4 was significantly inhibited by ketoconazole, causing almost no metabolism of parent UV-328 (Fig. 2B, Fig. S4B). Compared with Fig. 2A, almost all the mono-OH metabolites and di-OH metabolites were disappeared, indicating the predominant role of human CYP3A4 in the metabolism of UV-328.

3.4. Assignment of site of metabolism

Fig. 2A shows a typical UPLC chromatogram of UV-328 and its major metabolites. M20 has the largest peak area among all detected metabolites, suggesting that M20 is the dominant hydroxylated metabolite. To investigate the structural feature of hydroxylated metabolites of UV-328, we predicted the potential SoM on the basis of CYP-mediated oxidation using the combination of SMARTCyp and DFT calculation. SMARTCyp is the established cytochrome P450-mediated metabolism prediction server for the prediction of the SoM using a reactivity model (Rydberg et al., 2010). The CYP3A4-mediated oxidation occurred potentially at the benzene ring or at the alicyclic hydrocarbon of UV-328 (Fig. S5). The carbon atoms, C2, C16 and C22 have relatively low activation energies (75.9 kJ/mol, 75.9 kJ/mol, and 86.3 kJ/mol, respectively) that are required for Cpd I to react at individual carbon atoms. C2, C16 and C22 have the score of 67.74, 67.78, and 76.96, respectively. The lower score suggests a higher probability for individual carbon atoms to be the SoM. These three carbon atoms rank as the top three positions for CYP3A4-mediated hydroxylation reaction. The top-two ranked SoMs from SMARTCyp were reported to predict ~80% of the experimental SoMs (Rydberg et al., 2010). We further evaluated the activation energy of hydrogen abstraction from C-H bond of C2, C16 and C22 by Cpd I using DFT. During the process of CYP450-mediated hydroxylation reaction, the hydrogen abstraction from CH moiety by iron-bound oxygen atom of Cpd I is the first step followed by the formation of the $Fe^{IV}-OH$ intermediate by the radical reaction (Olsen et al., 2006). The calculated activation energy barrier for C2, C16 and C22 is 75.52 kJ/mol, 61.88 kJ/mol and 81.75 kJ/mol, respectively. The lower activation energy barrier means that the hydrogen free radical is easier to be abstracted by Cpd I, indicating a higher probability of SoM. The activation energies of C2 and C22 are very close to the estimated energies from SMARTCyp.

Based on the metabolites identified by UPLC-Q-TOF-MS/MS and the SoM by the *in silico* prediction, three mono-OH and three di-OH metabolites are proposed (Figs. 3 and 4). The mono-OH metabolites have three hydroxylation sites occurred at C2, C16 and C22. C16 has the lowest activation energy and the corresponding mono-OH metabolite may be dominant, thus M20 was suggested to be the metabolite following the hydroxylation at C16. The di-OH metabolites may also have three possible hydroxylation patterns occurred at C2 and C16, C2 and C22, or C16 and C22.

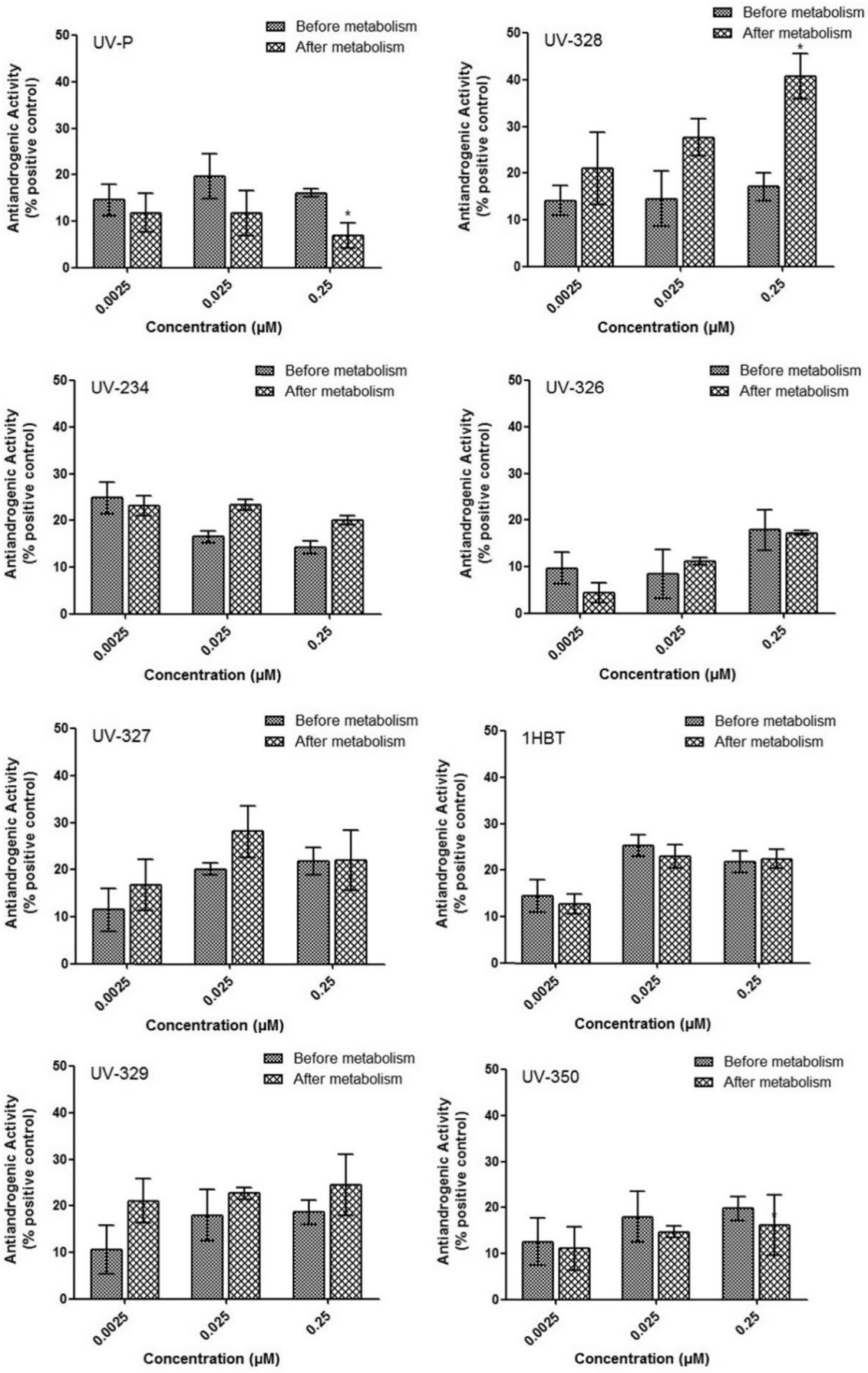

Fig. 1. Antiandrogenic activity was presented as percentage response, compared with the activity observed with 5×10^{-8} M dihydrotestosterone (DHT). * indicates $p < 0.05$ and means the significant difference between the androgenic activities before and after metabolism. All data were corrected with the appropriate blanks. Error bars stand for the standard deviation of each measurement.

Table 2
Human liver microsome-mediated hydroxylated metabolites of UV-328.

Reaction	Peak ID	Formula	m/z	R.T. (min)	Peak area	% Area	% Score
	UV-328	$C_{22}H_{29}N_3O$	352.2387	29.66	6.43e+05	6.6	90.4
Oxidation	M20	$C_{22}H_{29}N_3O_2$	368.2341	19.31	1.39e+06	14.1	93.4
	M24	$C_{22}H_{29}N_3O_2$	368.2341	21.19	3.85e+05	3.9	89.3
	M21	$C_{22}H_{29}N_3O_2$	368.2338	19.86	1.17e+05	1.2	86.6
Di-Oxidation	M5	$C_{22}H_{29}N_3O_3$	384.2286	9.41	8.47e+04	0.9	85.6
	M6	$C_{22}H_{29}N_3O_3$	384.2287	10.24	4.13e+05	4.2	85.8
	M11	$C_{22}H_{29}N_3O_3$	384.2284	10.45	6.72e+05	6.9	83.7

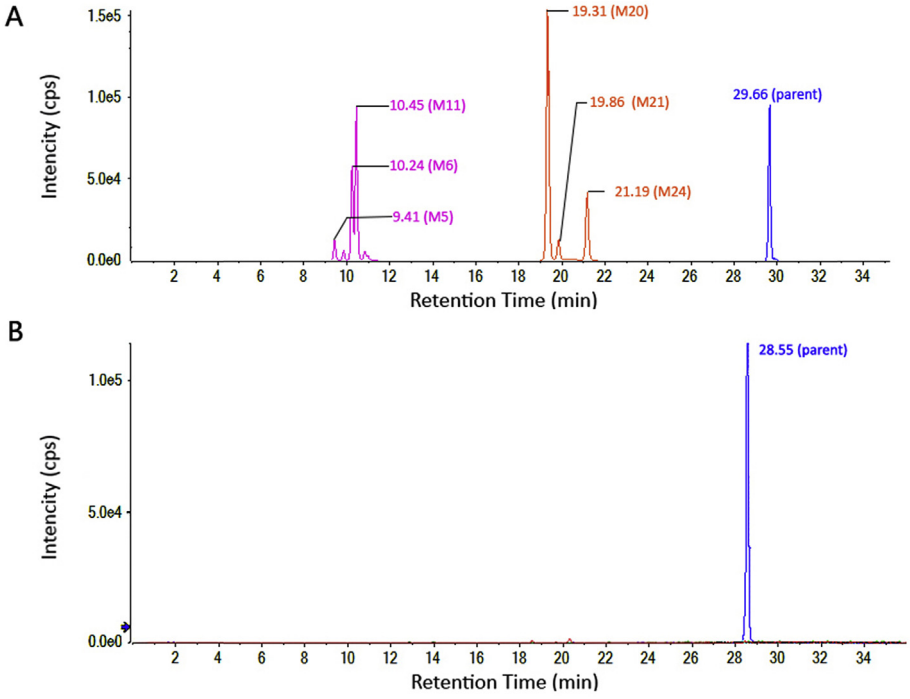

Fig. 2. Extracted ion chromatograms (EICs) of HLM-mediated metabolites of UV-328 (A) and the metabolites mediated by the incubation of HLM with CYP3A4 inhibitor ketoconazole (B).

4. Discussion

BUVSs are known to be metabolized by human CYP1A1 (Nagayoshi et al., 2015), however, whether human CYP3A4, the predominant enzyme among CYP450 family, can mediate the metabolism of BUVSs still remains unknown. Although UV-328 is generally considered persistent in the environment, our study revealed that it can be metabolized by human CYP3A4 into multiple products, among which, the mono-OH and di-OH metabolites are dominant. 1HBT was also reported to be degraded into major hydroxylated products such as 4-OH and 5-OH − 1HBT in an activated sludge system (Huntscha et al., 2014). Compared with the retention time at ~29.7 min for UV-328, the markedly shorter retention times of mono-OH metabolites and di-OH metabolites (19.31 min for M20, 21.19 min for M24, 19.86 min for M21, 9.54 min for M5, 10.24 min for M6, and 10.45 min for M11, Fig. 2) indicate the formation of less hydrophobic mono-OH or di-OH metabolites separated by ZorBax SB-C_{18} based reverse phase column.

Our study for the first time provided evidence on human CYP3A4-mediated metabolic activation of UV-328 and metabolic deactivation of UV-P toward human AR, suggesting the critical role of human CYP3A4-mediated biotransformation. BUVSs do not have any or a very weak AR disrupting effect at the low dose, but their potential toxicities after biotransformation could become alarming. UV-328 is one of the dominant BUVSs in fish, human urine, and breast milk (Kim et al., 2011; Lee et al., 2015; Naccarato et al., 2014). Its enhanced antiandrogenic activity after metabolism may potentially cause further adverse effects on sex differentiation in animal systems. Several sexual phenotypes have been reported to be caused by the exposure to androgenic disrupting chemicals (Gray et al., 1994). Therefore, future risk assessment of BUVSs as emerging contaminants should take full account of biotransformation products to assess their undesirable biological effects.

Our novel approach of the combined use of UPLC-Q-TOF-MS/MS for accurate molecular mass of metabolites and *in silico* prediction provides further insight into the metabolic activation of UV-328. Since the overall inhibition rate is as high as 40.7% for UV-328 at its initial concentration of 0.25 μM, it will also be interesting to determine which specific OH-UV-328 attributes to the observed metabolic activation. Further determination of their direct antiandrogenic effects requires the standards of OH-UV-328, which are not yet commercially available. Regardless, considering the multiple possible metabolites of UV-328 and their % areas, it becomes clear that the concentration of these metabolites likely approaches the environmentally relevant concentrations of approximately 0.01 mg/L. The enhanced toxicity observed in this study may result

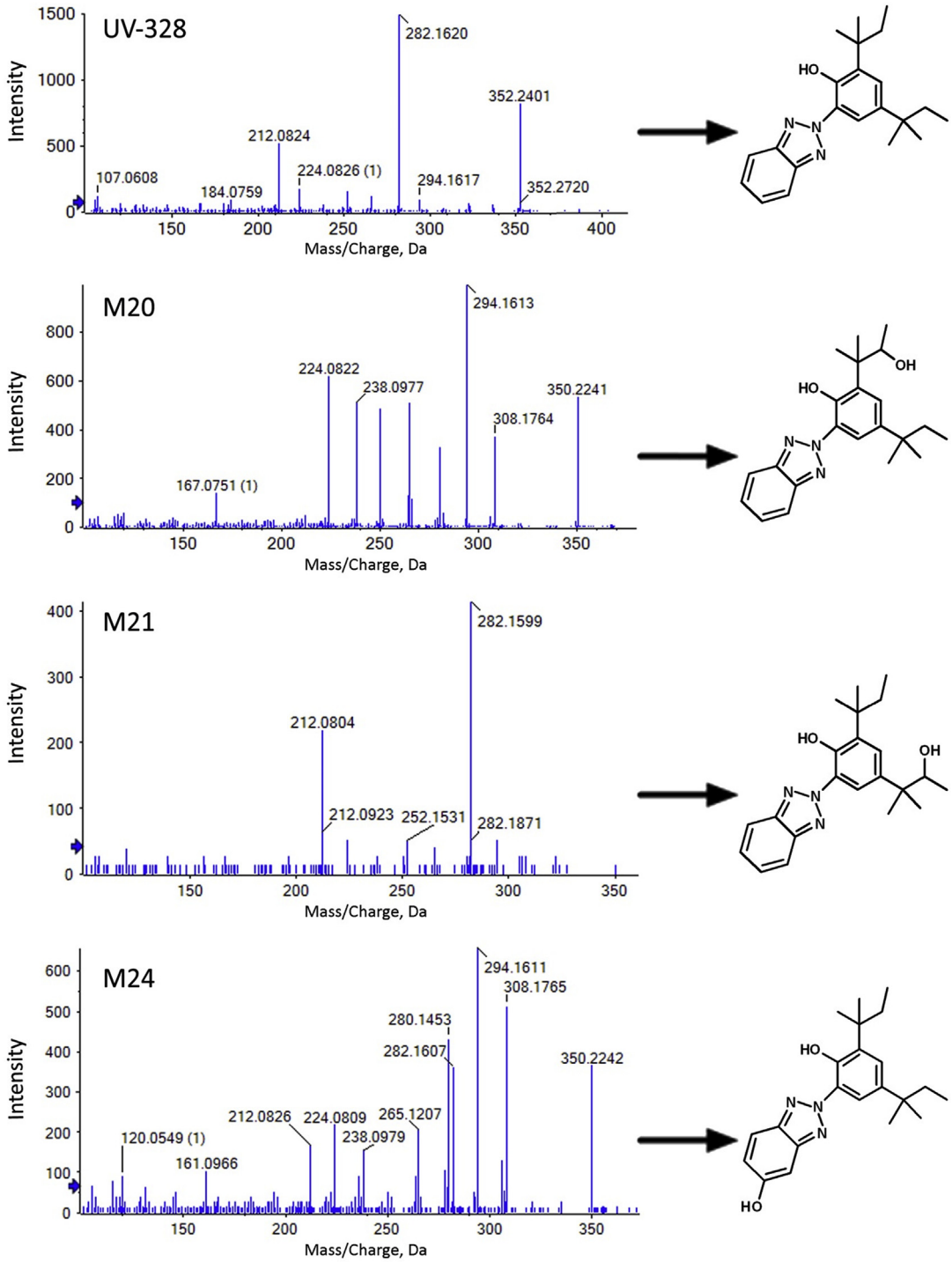

Fig. 3. The mass spectrum and structure of UV-328 and the proposed mono-OH metabolites, M20, M21 and M24.

from individual mono-OH/di-OH UV-328 metabolites or partly from the mixture toxicity effect. The role of aromatic hydroxylation in contributing to the enhanced toxicity has been documented for several structurally dissimilar groups of environmental contaminants. The molecular features susceptible to metabolic hydroxylation should be differentiated to cautiously prioritize the potential of BUVSs as emerging contaminants.

Our study further filled the knowledge gap that among eight tested BUVSs, only UV-328 and UV-P showed the significantly altered toxicity upon CYP3A4 mediated-metabolism. While the metabolites of UV-328 by human CYP3A significantly enhanced the antiandrogenic activity toward human AR, UV-P reduced the inhibition rate. An important environmental implication from this study is the fact that some, perhaps not all BUVSs may introduce secondary contaminants with an undesired exposure risk. Further research is warranted to decipher how the minute difference in structural moieties of BUVSs determines such a subtle difference in their biological activities.

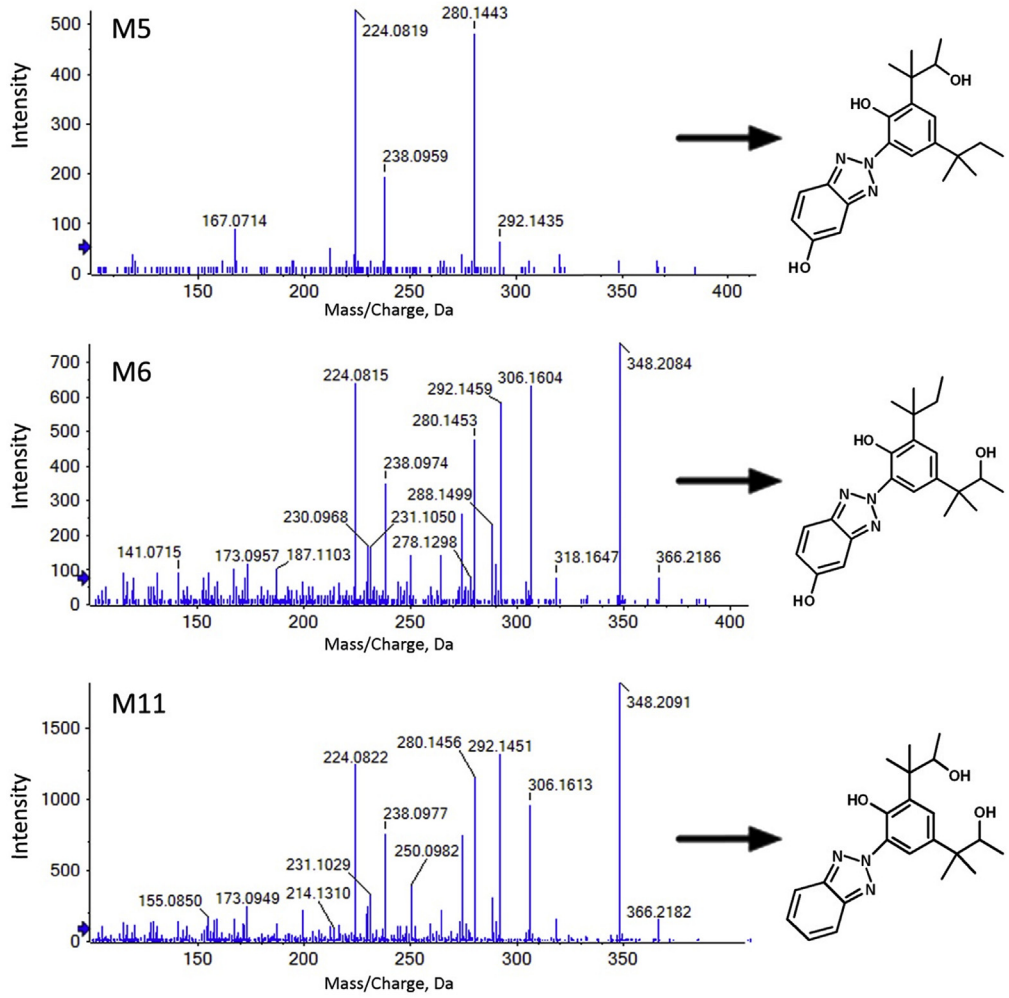

Fig. 4. The mass spectrum and proposed structures of di-OH metabolites of M5, M6 and M11.

Competing interests

The authors declare no competing financial interest.

Acknowledgements

The authors thank the National Natural Science Foundation of China (No. 21477113, 21277122), the Major Science and Technology Projects of Zhejiang Province (2014C03026), the financial support from Funds for International Cooperation and Exchange of the National Natural Science Foundation of China (21320102007), the Guangzhou Key Laboratory of Environmental Exposure and Health (No. GZKLEEH201605), and the Fundamental Research Funds for the Central Universities. CZ acknowledged the Welch Foundation for partial support.

Appendix A. Supplementary data

Supplementary data related to this article can be found at http://dx.doi.org/10.1016/j.envpol.2016.10.011.

References

Asimakopoulos, A.G., Wang, L., Thomaidis, N.S., Kannan, K., 2013a. Benzotriazoles and benzothiazoles in human urine from several countries: a perspective on occurrence, biotransformation, and human exposure. Environ. Int. 59, 274–281.

Asimakopoulos, A.G., Bletsou, A.A., Wu, Q., Thomaidis, N.S., Kannan, K., 2013b. Determination of 1,2,3-benzotriazoles and 1,3-benzothiazoles in human urine by liquid chromatography-tandem mass spectrometry. Anal. Chem. 85, 441–448.

Buser, H.R., Balmer, M.E., Schmid, P., Kohler, M., 2006. Occurrence of UV filters 4-methylbenzylidene camphor and octocrylene in fish from various swiss rivers with inputs from wastewater treatment plants. Environ. Sci. Technol. 40, 1427–1431.

Chen, R., Liu, C., Yuan, L.L., Zha, J.M., Wang, Z.J., 2016. 2, 4-Dichloro-6-nitrophenol, a photonitration product of 2, 4-dichlorophenol, caused antiandrogenic potency in Chinese rare minnows (*Gobiocypris rarus*). Environ. Pollut. 216, 591–598.

Fent, K., Chew, G., Li, J., Gomez, E., 2014. Benzotriazole UV-stabilizers and benzotriazole: antiandrogenic activity in vitro and activation of aryl hydrocarbon receptor pathway in zebrafish eleuthero-embryos. Sci. Total Environ. 482, 125–136.

Gray, L.E., Ostby, J.S., Kelce, W.R., 1994. Developmental effects of an environmental antiandrogen – the fungicide vinclozolin alters sex-differentiation of the male-rat. Toxicol. Appl. Pharmacol. 129, 46–52.

Harris, C.A., Routledge, E.J., Schaffner, C., Brian, J.V., Giger, W., Sumpter, J.P., 2007. Benzotriazole is antiestrogenic *in vitro* but not *in vivo*. Environ. Toxicol. Chem. 26, 2367–2372.

He, T.T., Liang, B., Liu, W.H., Shin, P.K.S., Wu, R.S.S., 2012. Estrogenic potential of benzotriazole on marine medaka (*Oryzias melastigma*). Ecotoxicol. Environ. Saf. 80, 327–332.

Huntscha, S., Hofstetter, T.B., Schymanski, E.L., Spahr, S., Hollender, J., 2014. Biotransformation of benzotriazoles: insights from transformation product identification and compound-specific isotope analysis. Environ. Sci. Technol. 48, 4435–4443.

Kameda, Y., Kimura, K., Miyazaki, M., 2011. Occurrence and profiles of organic sun-blocking agents in surface waters and sediments in Japanese rivers and lakes. Environ. Pollut. 159, 1570–1576.

Kawamura, Y., Ogawa, Y., Nishimura, T., Kikuchi, Y., Nishikawa, J., Nishihara, T., Tanamoto, K., 2003. Estrogenic activities of UV stabilizers used in food contact plastics and benzophenone derivatives tested by the yeast two-hybrid assay. J. Health Sci. 49, 205–212.

Kim, J.W., Isobe, T., Ramaswamy, B.R., Chang, K.H., Amano, A., Miller, T.M., Siringan, F.P., Tanabe, S., 2011. Contamination and bioaccumulation of benzotriazole ultraviolet stabilizers in fish from Manila Bay, the Philippines using an ultra-fast liquid chromatography-tandem mass spectrometry. Chemosphere 85, 751–758.

Lee, S., Kim, S., Park, J., Kim, H.J., Lee, J.J., Choi, G., Choi, S., Kim, S., Kim, S.Y., Choi, K., Kim, S., Moon, H.B., 2015. Synthetic musk compounds and benzotriazole ultraviolet stabilizers in breast milk: occurrence, time-course variation and infant health risk. Environ. Res. 140, 466–473.

LeFevre, G.H., Muller, C.E., Lo, R.J.X., Luthy, R.G., Sattely, E.S., 2015. Rapidphytotransformation of benzotriazole generates synthetic tryptophan and auxin analogs in arabidopsis. Environ. Sci. Technol. 49, 10959–10968.

LeFevre, G.H., Portmann, A.C., Muller, C.E., Sattely, E.S., Luthy, R.G., 2016. Plant assimilation kinetics and metabolism of 2-mercaptobenzothiazole tire rubber vulcanizers by arabidopsis. Environ. Sci. Technol. 50, 6762–6771.

Li, F., Xie, Q., Li, X.H., Li, N., Chi, P., Chen, J.W., Wang, Z.J., Hao, C., 2010. Hormone activity of hydroxylated polybrominated diphenyl ethers on human thyroid receptor-beta: in vitro and in silico investigations. Environ. Health Perspect. 118, 602–606.

Li, J., Chen, M., Wang, Z.J., Ma, M., Peng, X.Z., 2011. Analysis of environmental endocrine disrupting activities in wastewater treatment plant effluents using recombinant yeast assays incorporated with exogenous metabolic activation system. Biomed. Environ. Sci. 24, 132–139.

Li, J., Li, N., Ma, M., Giesy, J.P., Wang, Z.J., 2008. In vitro profiling of the endocrine disrupting potency of organochlorine pesticides. Toxicol. Lett. 183, 65–71.

Liu, Y.S., Ying, G.G., Shareef, A., Kookana, R.S., 2011. Biodegradation of three selected benzotriazoles under aerobic and anaerobic conditions. Water Res. 45, 5005–5014.

Liu, Y.S., Ying, G.G., Shareef, A., Kookana, R.S., 2012. Occurrence and removal of benzotriazoles and ultraviolet filters in a municipal wastewater treatment plant. Environ. Pollut. 165, 225–232.

Liu, R.Z., Ruan, T., Wang, T., Song, S.J., Guo, F., Jiang, G.B., 2014. Determination of nine benzotriazole UV stabilizers in environmental water samples by automated online solid phase extraction coupled with high-performance liquid chromatography-tandem mass spectrometry. Talanta 120, 158–166.

Lu, Z., Kania-Korwel, I., Lehmler, H.J., Wong, C.S., 2013. Stereoselective formation of mono- and dihydroxylated polychlorinated biphenyls by rat cytochrome P450 2B1. Environ. Sci. Technol. 47, 12184–12192.

Ma, M., Li, J., Wang, Z.J., 2005. Assessing the detoxication efficiencies of wastewater treatment processes using a battery of bioassays/biomarkers. Arch. Environ. Contam. Toxicol. 49, 480–487.

Miller, D., Wheals, B.B., Beresford, N., Sumpter, J.P., 2001. Estrogenic activity of phenolic additives determined by an in vitro yeast bioassay. Environ. Health Perspect. 109, 133–138.

Morohoshi, K., Yamamoto, H., Kamata, R., Shiraishi, F., Koda, T., Morita, M., 2005. Estrogenic activity of 37 components of commercial sunscreen lotions evaluated by in vitro assays. Toxicol. In Vitro 19, 457–469.

Naccarato, A., Gionfriddo, E., Sindona, G., Tagarelli, A., 2014. Simultaneous determination of benzothiazoles, benzotriazoles and benzosulfonamides by solid phase microextraction-gas chromatography-triple quadrupole mass spectrometry in environmental aqueous matrices and human urine. J. Chromatogr. A 1338, 164–173.

Nagayoshi, H., Kakimoto, K., Takagi, S., Konishi, Y., Kajimura, K., Matsuda, T., 2015. Benzotriazole ultraviolet stabilizers show potent activities as human aryl hydrocarbon receptor ligands. Environ. Sci. Technol. 49, 578–587.

Nakata, H., Murata, S., Filatreau, J., 2009. Occurrence and concentrations of benzotriazole UV stabilizers in marine organisms and sediments from the Ariake sea, Japan. Environ. Sci. Technol. 43, 6920–6926.

Olsen, L., Rydberg, P., Rod, T.H., Ryde, U., 2006. Prediction of activation energies for hydrogen abstraction by cytochrome P450. J. Med. Chem. 49, 6489–6499.

Ruan, T., Liu, R.Z., Fu, Q., Wang, T., Wang, Y.W., Song, S.J., Wang, P., Teng, M., Jiang, G.B., 2012. Concentrations and composition profiles of benzotriazole UV stabilizers in municipal sewage sludge in China. Environ. Sci. Technol. 46, 2071–2079.

Rydberg, P., Gloriam, D.E., Zaretzki, J., Breneman, C., Olsen, L., 2010. SMARTCyp: a 2D method for prediction of cytochrome P450-mediated drug metabolism. ACS Med. Chem. Lett. 1, 96–100.

Seeland, A., Oetken, M., Kiss, A., Fries, E., Oehlmann, J., 2012. Acute and chronic toxicity of benzotriazoles to aquatic organisms. Environ. Sci. Pollut. 19, 1781–1790.

Tsui, M.M., Leung, H.W., Lam, P.K., Murphy, M.B., 2014. Seasonal occurrence, removal efficiencies and preliminary risk assessment of multiple classes of organic UV filters in wastewater treatment plants. Water Res. 53, 58–67.

Wang, L., Asimakopoulos, A.G., Moon, H.B., Nakata, H., Kannan, K., 2013. Benzotriazole, benzothiazole, and benzophenone compounds in indoor dust from the United States and East Asian countries. Environ. Sci. Technol. 47, 4752–4759.

Wang, L., Asimakopoulos, A.G., Kannan, K., 2015. Accumulation of 19 environmental phenolic and xenobiotic heterocyclic aromatic compounds in human adipose tissue. Environ. Int. 78, 45–50.

Wick, A., Jacobs, B., Kunkel, U., Heininger, P., Ternes, T.A., 2016. Benzotriazole UV stabilizers in sediments, suspended particulate matter and fish of German rivers: new insights into occurrence, time trends and persistency. Environ. Pollut. 212, 401–412.

Yoshihara, S., Makishima, M., Suzuki, N., Ohta, S., 2001. Metabolic activation of bisphenol A by rat liver S9 fraction. Toxicol. Sci. 62, 221–227.

Zhang, J., Kamstra, J.H., Ghorbanzadeh, M., Weiss, J.M., Hamers, T., Andersson, P.L., 2015. In silico approach to identify potential thyroid hormone disruptors among currently known dust contaminants and their metabolites. Environ. Sci. Technol. 49, 10099–10107.